

# Critical behavior of 2 and 3 dimensional ferro- and antiferromagnetic spin ice systems in the framework of the Effective Field Renormalization Group technique

Angel J. Garcia-Adeva\* and David L. Huber

*Department of Physics; University of Wisconsin–Madison; Madison, WI 53706*

In this work we generalize and subsequently apply the Effective Field Renormalization Group technique to the problem of ferro- and antiferromagnetically coupled Ising spins with local anisotropy axes in geometrically frustrated geometries (*kagomé* and pyrochlore lattices). In this framework, we calculate the various ground states of these systems and the corresponding critical points. Excellent agreement is found with exact and Monte Carlo results. The effects of frustration are discussed. As pointed out by other authors, it turns out that the spin ice model can be exactly mapped to the standard Ising model but with effective interactions of the opposite sign to those in the original Hamiltonian. Therefore, the ferromagnetic spin ice is frustrated, and does not order. Antiferromagnetic spin ice (in both 2 and 3 dimensions), is found to undergo a transition to a long range ordered state. The thermal and magnetic critical exponents for this transition are calculated. It is found that the thermal exponent is that of the Ising universality class, whereas the magnetic critical exponent is different, as expected from the fact that the Zeeman term has a different symmetry in these systems. In addition, the recently introduced Generalized Constant Coupling method is also applied to the calculation of the critical points and ground state configurations. Again, a very good agreement is found with both exact, Monte Carlo, and renormalization group calculations for the critical points. Incidentally, we show that the generalized constant coupling approach can be regarded as the lowest order limit of the EFRG technique, in which correlations outside a frustrated unit are neglected, and scaling is substituted by strict equality of the thermodynamic quantities.

PACS numbers: 75.10.Hk, 75.25.+z, 75.40.Cx

## I. INTRODUCTION

Geometrically frustrated antiferromagnets (GFAF) have emerged in the last years as a new class of magnetic materials with many unusual physical properties<sup>1,2,3,4</sup>. In these materials, the elementary magnetic unit is the triangle, which makes it impossible to satisfy all the antiferromagnetic bonds at the same time, with the result of a macroscopically degenerate ground state. Examples of GFAF are the pyrochlore and the *kagomé* lattices. In the former, the magnetic ions occupy the corners of a 3D arrangement of corner sharing tetrahedra; in the later, the magnetic ions occupy the corners of a 2D arrangement of corner sharing triangles (see Fig. 1). In the case of materials which crystallize in the pyrochlore structure, the static magnetic susceptibility follows the Curie–Weiss law down to temperatures well below the Curie–Weiss temperature. At this point, usually one to two orders of magnitude smaller than the Néel point predicted by the standard mean field (MF) theory, some systems exhibit some kind of long range order (LRO), whereas others show a transition to a spin glass state (SG). This is a striking feature for a system with only a marginal

amount of disorder. Finally, there are some pyrochlores which do not exhibit any form of order whatsoever, and are usually regarded as spin liquids. In the case of the *kagomé* lattice, even though there are very few real systems where this structure is realized, the magnetic properties fall in two major categories: the vast majority of the compounds studied show a transition to a LRO state with a non collinear configuration of spins, and a few systems exhibit no LRO, but a SG like transition.

Surprisingly, Harris and coworkers<sup>5,6,7</sup> recently showed that geometrical frustration can also arise from ferromagnetic interactions. This cannot occur for Heisenberg spins but, in some cases, a strong single ion anisotropy along high symmetry directions of the crystallographic structure can force the spins to point in such directions, so they can effectively be considered as Ising spins<sup>8</sup>. In this case, the Ising spins with ferromagnetic interactions do not order at any finite temperature. They analyzed this problem in the context of Ising spins in the corners of a pyrochlore lattice, and termed this system spin ice pyrochlore, because it can be mapped to the well know proton ordering problem in the ice lattice. Furthermore, in full equivalence with the ice problem, the spin ice model presents a slow dynamic, due to the existence of large energy barriers associated with rearrangements of the spins in the ground state, resulting in a spin freezing which resembles a spin glass, *but occurring in a system where chemical disorder is absent*<sup>5,9</sup>.

While at first sight this can look like a very interesting academic problem, it turned out to be also of enormous practical interest, because various pyrochlore oxides were found to have strong single ion anisotropy along the  $\langle 111 \rangle$ -directions of the lattice. This effect usually occurs for rare earth magnetic ions with a large orbital moment, as it is the case of the pyrochlores  $\text{Ho}_2\text{Ti}_2\text{O}_7$ ,  $\text{Dy}_2\text{Ti}_2\text{O}_7$ , and  $\text{Yb}_2\text{Ti}_2\text{O}_7$ , among others, which are now known to be very good realizations of the spin ice model.

From the theoretical point of view, apart from the interest of the spin ice system itself, this system also offers a unique opportunity for testing models which incorporate geometrical frustration, for the obvious reason that the Ising Hamiltonian is simpler to study mathematically than the Heisenberg one and, in some cases, analytical results are easily obtained, which can be readily compared with experimental data or simulations. If such a comparison is adequate, one can get some confidence that these techniques can also be applied to the Heisenberg problem in the pyrochlore lattice, which is an even more interesting problem.

This is precisely the purpose of the present work. We will study the critical properties of geometrically frustrated Ising *ferro-* and *antiferromagnets* by introducing a generalization of a well known real space renormalization group technique, the so called Effective Field Renormalization Group (EFRG) method<sup>10,11</sup>, which has been successfully applied to a large variety of systems (see Ref. 12 and references therein), and it is known to provide very good estimates of the critical temperature and the critical exponents. We apply this technique to two model systems: the spin ice problem in the pyrochlore lattice, and a 2D analog to the spin ice problem, which consists of Ising spins in the *kagomé* lattice with local axes of anisotropy along the heights of the triangle. This second example, though academic, is a very instructive one, as it will serve as an example to develop the present method. Our first task will be to generalize the EFRG technique to include the effect of geometrical frustration, that is, the non-Bravais character of the lattices considered. We will then study the existence of critical points and their values for both ferro- and antiferromagnetic interactions. The obtained values are compared with exact values known for the Ising model in the *kagomé* lattice<sup>13</sup> and with numerical estimations of this quantity obtained by Harris and Bramwell for the spin ice pyrochlore<sup>7</sup>. We find that, even at the lowest order of approximation, in which correlations with ions further than NN are neglected, the estimates are excellent for both lattices. Furthermore, we show that these spin ice-like Ising models can be related to the standard Ising model<sup>31</sup>. Therefore, we are able to understand why the ground state given by the ice rules is never

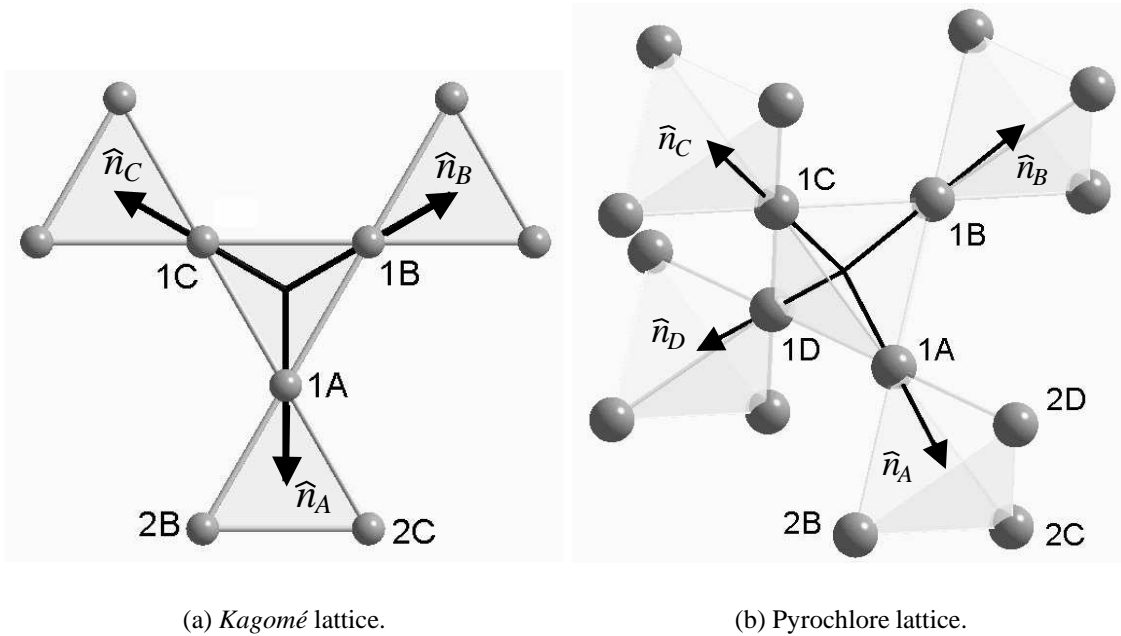


FIG. 1: The structures considered in this work. The black thick lines indicate the axes of anisotropy. Spin labels are of the form  $i\alpha$ , where  $\alpha$  is the label of the sublattice and  $i$  the index of the spin inside the corresponding sublattice. The normal vectors  $\hat{n}_\alpha$  have been also depicted.

found in these systems, in agreement with numerical evidences provided by other authors<sup>7,9</sup>. Next, we evaluate the thermal and magnetic exponents for the transition to an ordered state that is found for antiferromagnetic spin ice, namely, a ground state in which all the spins point out or all the spins point in. These exponents are calculated for two limiting cases: the one corresponding to Ising spins with a single anisotropy axis, that is, the standard Ising model, and the one corresponding to the spin problem. For the standard Ising model the calculated exponents are found to be in good agreement when compared with exact values for 2D lattices, and with Monte Carlo simulations for the 3D lattice, for the Ising universality class. For the spin ice case, the thermal exponent is the same as in the standard Ising model, whereas the magnetic one is found to be different for both lattices, in agreement with the fact that the Zeeman term in this case does not have the same symmetry as in the standard Ising model.

Additionally, we find interesting to compare the results obtained from this new method with the ones predicted by the Generalized Constant Coupling (GCC) model, recently developed by the present authors<sup>14,15</sup>, which has been shown to provide very accurate results for the magnetic properties of Heisenberg GFAF. The results for the critical points and ground state configurations obtained in the GCC framework are found to be in excellent agreement with the ones found by using the EFRG technique, in spite of the mathematical simplicity of the GCC method. Incidentally, we show that this agreement is not a coincidence, but it is related to the fact that the GCC method can be considered as the zero-th order approximation of the EFRG scheme.

The remainder of this paper is organized as follows: in the next section, we introduce the systems we will deal with and a brief summary of the EFRG method, together with the corresponding generalization to deal with geometrically frustrated lattices. In the third section we develop the EFRG scheme for both the *kagomé* and pyrochlore lattice with anisotropic Ising interactions. In section IV, the finite scaling hypothesis is used to calculate the non-trivial fixed points of the RG

transformation (the critical points), together with the possible ground state configurations of the system. In section V we calculate the thermal and magnetic critical exponents for the long range ordered state found in the previous section for antiferromagnetic interactions. In section VI, we apply the GCC model to the present problem and, again, the critical points and ground state configurations are calculated and compared with the EFRG method. In section VII, the connection between both schemes is furnished. Finally, section VIII is devoted to the conclusions.

## II. STATEMENT OF THE PROBLEM

In the systems we will consider below, the strong single-ion anisotropy forces the spins in the lattice to point in high symmetry directions and, to a first approximation, they can be regarded as Ising spins<sup>8</sup>. For example, in the spin ice pyrochlore, each ion in the elementary tetrahedral unit points in a different  $\langle 111 \rangle$ -type direction, which connects the spin with the center of the tetrahedra. Therefore, the spin variables are not scalar ones, but have vectorial character. We will represent each of the spins by a vector  $\vec{s}_{i\alpha} = s_{i\alpha} \hat{n}_\alpha$ , where  $s_{i\alpha}$  takes the values  $\pm 1$  and  $\hat{n}_\alpha$  stands for the unitary vector in one of the directions of anisotropy, where  $\alpha$  takes the values  $\alpha = A, B, C, \dots$ , depending on the number of different directions of anisotropy (see Fig. 1). The index  $i$  runs over all the spins with a given normal vector.

The Ising Hamiltonian with only NN interactions in  $d$ -dimensional units can be then put as

$$\mathcal{H} = K \sum_{\alpha \neq \beta} \sum_{\langle i, j \rangle} \vec{s}_{i\alpha} \cdot \vec{s}_{j\beta}, \quad (1)$$

where  $K = \beta J$  is the  $d$ -dimensional coupling constant, which is positive for ferromagnetic interactions and negative for antiferromagnetic interactions. We can see that, in this way, we have defined a finite number of sublattices, characterized by the corresponding orientation of the Ising spins, which has the advantage that a spin in sublattice  $\alpha$  interacts only with spins in different sublattices.

The geometries we will consider in this work are those depicted in Fig. 1: anisotropic Ising spins in the *kagomé* lattice, which can be considered as a 2D analog to the spin ice problem, and the spin ice problem, that is, anisotropic Ising spins in a pyrochlore lattice.

In order to study the critical properties of these systems, we will make use of the so called EFRG technique, which has been proved to be a very good RG scheme for dealing with critical phenomena. We will not present the method here, as there is an excellent review on this subject<sup>12</sup>, but only the most important notions.

According to the idea of scaling<sup>16</sup>, close to the transition the singular part of the free energy scales as

$$f_s(\epsilon, H) = l^{-d} f_s(l^{1/\nu} \epsilon, l^{y_H} H), \quad (2)$$

where  $\epsilon = K - K_c$ , with  $K_c$  the critical coupling,  $l$  is an arbitrary scaling factor,  $d$  is the dimensionality of the lattice,  $y_H$  is the magnetic critical exponent and  $H$  the applied magnetic field, and  $\nu$  is the correlation length critical exponent. Any other thermodynamic quantity,  $P$ , can be evaluated as derivatives of this singular part of the free energy near the transition, and will behave as a power law

$$P \sim |\epsilon|^{-\sigma}, \quad (3)$$

where  $\sigma$  is the critical exponent of the quantity  $P$ . For example, the magnetization, near criticality, behaves as

$$m(\epsilon, H) = l^{-d+y_H} m(l^{1/\nu} \epsilon, l^{y_H} H). \quad (4)$$

On the other hand, according to the finite size scaling hypothesis, the generalized scaling relation obeyed by any thermodynamic quantity  $P$ , taking into account the finite size  $L$  of the system, can be put as<sup>16</sup>

$$P(\epsilon, H, L) = l^\phi P(l^{1/\nu} \epsilon, l^{y_H} H, l^{-1} L), \quad (5)$$

where  $\phi = \sigma/\nu$  is the anomalous dimension of the quantity  $P$ . By choosing a smaller system of size  $L'$ , fixing the scaling factor to the value  $l = \frac{L}{L'}$ , and introducing the variables  $\epsilon' = l^{1/\nu} \epsilon = K' - K_c$  and  $H' = l^{y_H} H$ , we can rewrite relation (5) in the form

$$\frac{P_{L'}(K', H')}{L'^\phi} = \frac{P_L(K, H)}{L^\phi}. \quad (6)$$

This is the basic equation from where a mapping  $(K, H) \rightarrow (K', H')$  can be established, and the corresponding critical points and exponents obtained.

By applying relation (6) to different thermodynamic quantities, different RG approaches are generated. For example, on applying (6) to the correlation length, we have

$$\frac{\xi'(K', H')}{L'} = \frac{\xi(K, H)}{L}, \quad (7)$$

which means that, for the correlation length, the anomalous dimension is the unity.

The EFRG approach corresponds to apply relation (6) to the order parameter (magnetization). The order parameter for two clusters of different size is calculated by using the Callen–Suzuki identity<sup>17,18</sup>

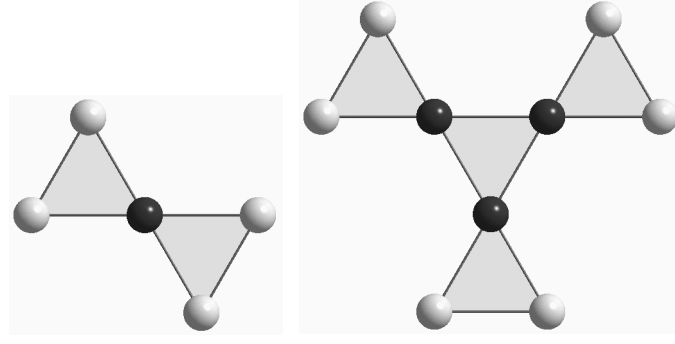
$$\langle O_p \rangle = \left\langle \frac{\text{Tr}_p O_p e^{\mathcal{H}_p}}{\text{Tr}_p e^{\mathcal{H}_p}} \right\rangle_{\mathcal{H}}, \quad (8)$$

where the partial trace is taken over the set of  $p$  spin variables specified by the finite size cluster Hamiltonian  $\mathcal{H}_p$ ;  $O_p$  is the corresponding order parameter, and  $\langle \dots \rangle_{\mathcal{H}}$  indicates the usual canonical thermal average over the ensemble defined by the complete Hamiltonian  $\mathcal{H}$ . The idea is then to replace the effect of the total Hamiltonian not included in the partial trace in (8) by fixed values of the magnetization of the ions outside the cluster, which act as a symmetry breaking field,  $b$ . In this way, the order parameter in the finite cluster can be computed for  $b \ll 1$  and  $H \ll 1$ , and an equation of the form

$$m_p(K, b, H) = \langle O_p \rangle = f_p(K) b + g_p(K) H, \quad (9)$$

is obtained. Repeating the same calculation for a cluster of different size,  $p'$ , and assuming that both magnetizations are related by the scaling relation (4) near criticality, we obtain the following equation

$$f_{p'}(K') b' + g_{p'}(K') H' = l^{d-y_H} f_p(K) b + l^{d-y_H} g_p(K) H. \quad (10)$$



(a) 1-spin cluster.

(b) 3-spins cluster.

FIG. 2: Clusters used in this work for the *kagomé* lattice. Dark spheres represent spins belonging to the cluster itself and white spheres the corresponding surrounding sites (those creating an effective field).

As  $b$  and  $b'$  are, in some sense, magnetizations, they are also assumed to satisfy (4), so we have the following relation

$$f_{p'}(K') = f_p(K), \quad (11)$$

from which the fixed points of this RG transformation and, thus the critical points, are found by solving this equation for  $K' = K = K_c$ . The corresponding thermal eigenvalue is obtained as the corresponding eigenvalue of this recursion relation, linearized near the critical point

$$\lambda_T = \left. \frac{\partial f_p}{\partial K} \left( \frac{\partial f_{p'}}{\partial K'} \right)^{-1} \right|_{K_c}, \quad (12)$$

and by making use of (7) together with the definition  $\lambda_T = l^{y_T} = l^{1/\nu}$ , we can calculate the correlation length critical exponent as

$$\nu = \frac{1}{y_T} = \frac{\ln l}{\ln \lambda_T}. \quad (13)$$

The magnetic critical exponent is calculated from

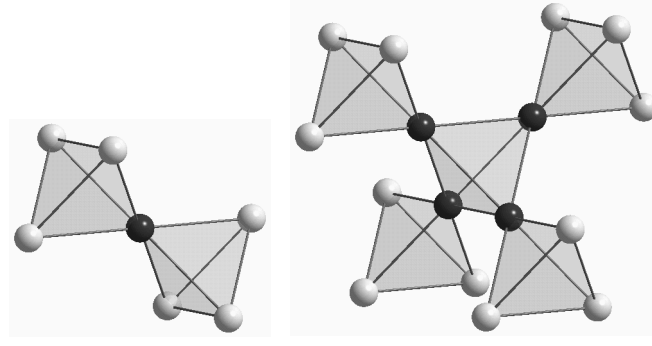
$$g_{p'}(K') H' = l^{d-y_H} g_p(K) H, \quad (14)$$

together with the scaling relation for the magnetic fields,  $H' = l^{y_H} H$ , as

$$y_H = \frac{1}{2} \left( d + \frac{1}{\ln l} \ln \frac{g_p(K_c)}{g_{p'}(K_c)} \right). \quad (15)$$

The only source of inaccuracy in these relations is in the finite sizes of the clusters. However, it has been found that these kinds of approaches are applicable to rather small systems and, sometimes, they are even more accurate than other RG approaches, for clusters of adequate size<sup>12</sup>.

Even though the EFRG scheme has been successfully applied to a broad range of problems, the original formulation of this method is not well suited to deal with the effects of geometrical



(a) 1-spin cluster.

(b) 4-spins cluster.

FIG. 3: Clusters used in this work for the pyrochlore lattice. Dark spheres represent spins belonging to the cluster itself and white spheres the corresponding surrounding sites (those creating an effective field).

frustration, that is, magnetic systems with a non-Bravais lattice, as those considered in this work. Therefore, our first task, is to generalize this technique to include this class of systems. In order to accomplish this goal, we must face two problems: on one hand, due to the non-Bravais character of the lattices, we cannot characterize the full system with only one order parameter; on the other hand, the finite clusters considered have to have a minimum size such that all the order parameters variables are included in the reduced trace, at least for one of the clusters, which involves a more complicated mathematical problem. These difficulties, of course, are not a particular flaw of the EFRG scheme, as they are present in all the real space RG schemes, and are related to the fact that non-Bravais lattices are non-invariant under a scale transformation. To cite an example, under a block transformation, the *kagomé* lattice does not transform in itself, but in a triangular lattice.

The easiest way of solving these technical difficulties is by subdividing the non-Bravais lattice in a number of Bravais lattices, and allowing for a different order parameter in each sublattice. For example, in the case of the *kagomé* lattice, it can be considered as formed by  $n = 3$  interlocked triangular lattices ( $\alpha = A, B, C$ ), whereas in the pyrochlore case, it can be considered as formed by  $n = 4$  interlocked FCC lattices ( $\alpha = A, B, C, D$ ).

Next, we have to decide the size of the two finite clusters we are considering. The most obvious choice is to consider a cluster formed by one single spin and another one formed by  $p = 3$  spins for the *kagomé* lattice (see Fig. 2) and  $p = 4$  spins for the pyrochlore lattice (see Fig. 3).

The following step is to evaluate the expectation value of each of the order parameters for these clusters by using the Callen–Suzuki identity, a task that we carry out in the next section.

### III. EVALUATION OF THE ORDER PARAMETERS

#### A. 1-spin cluster order parameter

Let us consider the cluster defined by the ion 1 in sublattice  $\alpha$ . The Hamiltonian of this cluster is given by

$$\mathcal{H}_{1\alpha} = K' \vec{s}_{1\alpha} \sum_{\beta \neq \alpha} \sum_i^z \vec{s}_{i\beta} = \vec{s}_{1\alpha} \cdot \vec{\xi}_{1\alpha}, \quad (16)$$

where the subindex  $1\alpha$  makes reference to the fact that the Hamiltonian corresponds to a cluster of 1 spin belonging to sublattice  $\alpha$ , and  $\vec{\xi}_{1\alpha}$  stands for the symmetry breaking field acting on the spin of the 1-spin cluster, which belong to sublattice  $\alpha$ . The sum over the  $i$  index is performed over the NN of the  $1\alpha$  spin, with  $z$  the number of NN in each of the sublattices ( $z = 2$  for both the *kagomé* and pyrochlore lattices). By using the Callen–Suzuki identity we can calculate the order parameter in sublattice  $\alpha$  for a cluster formed by 1 spin

$$\vec{m}_{1\alpha} = \langle \vec{s}_{1\alpha} \rangle = \left\langle \frac{Tr_{1\alpha} \vec{s}_{1\alpha} e^{\mathcal{H}_{1\alpha}}}{Tr_{1\alpha} e^{\mathcal{H}_{1\alpha}}} \right\rangle_{\mathcal{H}}. \quad (17)$$

As commented above,  $Tr_{1\alpha}$  represents the partial trace with respect to the variables of the spin  $1\alpha$ , and the symbol  $\langle \dots \rangle_{\mathcal{H}}$  stands for the usual canonical thermal average taken over the ensemble defined by the complete Hamiltonian  $\mathcal{H}$ . This equation can be put in the more convenient form

$$m_{1\alpha}^{\mu} = \left\langle \frac{\partial}{\partial \xi_{1\alpha}^{\mu}} \ln Tr_{1\alpha} e^{\mathcal{H}_{1\alpha}} \right\rangle_{\mathcal{H}}, \quad (18)$$

where  $a^{\mu}$  stands for the  $\mu$ -th component of the vector  $\vec{a}$ . A simple calculation yields

$$\vec{m}_{1\alpha} = \hat{n}_{\alpha} \left\langle \tanh \left( \hat{n}_{\alpha} \cdot \vec{\xi}_{1\alpha} \right) \right\rangle_{\mathcal{H}}. \quad (19)$$

Next, we make use of the operator identity<sup>19</sup>

$$f(x + a) = e^{a D_x} f(x), \quad (20)$$

where  $D_x = \frac{\partial}{\partial x}$ , to rewrite eq. (19) in the more convenient form

$$\vec{m}_{1\alpha} = \hat{n}_{\alpha} \left\langle e^{\hat{n}_{\alpha} \cdot \vec{\xi}_{1\alpha} D_x} \right\rangle_{\mathcal{H}} \tanh x|_{x=0}. \quad (21)$$

Finally, by making use of the van der Waerden identity

$$e^{aS} = \cosh a + S \sinh a, \quad S = \pm 1, \quad (22)$$

we can put

$$e^{\hat{n}_{\alpha} \cdot \vec{\xi}_{1\alpha} D_x} = \exp \left[ K' \hat{n}_{\alpha} \cdot \sum_{\beta \neq \alpha} \sum_i^z \vec{s}_{i\beta} D_x \right] = \prod_{\beta \neq \alpha} \prod_i^z [\rho_x + s_{i\beta} \nu_x], \quad (23)$$

where  $\rho_x = \cosh(\mathcal{K}' D_x)$  and  $\nu_x = \sinh(\mathcal{K}' D_x)$ , with  $\mathcal{K}' = K' \cos \theta = K' \hat{n}_{\alpha} \cdot \hat{n}_{\beta}$ . The expression of  $\mathcal{K}'$  takes into account the fact that, for the structures considered in this work, the angle between the directions of anisotropy is the same for any pair of neighboring spins.

Then, the order parameter for the 1-spin cluster can be put in the form

$$\vec{m}_{1\alpha} = \hat{n}_{\alpha} \left\langle \prod_{\beta \neq \alpha} \prod_i^z [\rho_x + s_{i\beta} \nu_x] \right\rangle_{\mathcal{H}} \tanh x|_{x=0}. \quad (24)$$



For example, for the *kagomé* lattice, the previous expression takes the form

$$\begin{aligned} \vec{m}_{1\alpha} = \hat{n}_\alpha & \left[ 2\rho_x^3 \nu_x (\langle s_{1\beta} \rangle_{\mathcal{H}} + \langle s_{1\gamma} \rangle_{\mathcal{H}}) \right. \\ & + \rho_x^2 \nu_x^2 (\langle s_{1\beta} s_{2\beta} \rangle_{\mathcal{H}} + \langle s_{1\gamma} s_{2\gamma} \rangle_{\mathcal{H}} + 2 \langle s_{1\beta} s_{1\gamma} \rangle_{\mathcal{H}} + 2 \langle s_{1\beta} s_{2\gamma} \rangle_{\mathcal{H}}) \\ & \left. + 2\rho_x \nu_x^3 (\langle s_{1\beta} s_{1\gamma} s_{2\gamma} \rangle_{\mathcal{H}} + \langle s_{1\beta} s_{1\gamma} s_{2\beta} \rangle_{\mathcal{H}}) + \nu_x^4 \langle s_{1\beta} s_{1\gamma} s_{2\beta} s_{2\gamma} \rangle_{\mathcal{H}} \right] \tanh x|_{x=0}, \\ & (\alpha \neq \beta \neq \gamma). \end{aligned} \quad (25)$$

These kind of equations, though exact, are intractable, and we have to resort to some kind of approximation. The simplest one corresponds to neglect 2-spin and higher order correlations<sup>19</sup>, that is

$$\langle s_{i\alpha} s_{j\beta} \dots s_{k\gamma} \rangle_{\mathcal{H}} \simeq \langle s_{i\alpha} \rangle_{\mathcal{H}} \langle s_{j\beta} \rangle_{\mathcal{H}} \dots \langle s_{k\gamma} \rangle_{\mathcal{H}}, \quad (26)$$

which is equivalent to neglect terms of the order of  $K_c^2$  and higher in the calculation of the critical points. It must be noted, however, that this approximation is superior to the standard MF theory, since it takes exactly into account the relation  $\langle s_{i\beta}^2 \rangle = 1$  ( $i \neq 1$ ), through the van der Waerden identity.

Applying (26) to (24), and to first order in  $\langle s_{i\alpha} \rangle_{\mathcal{H}} = b_{1\alpha}$  (which constitutes a good approximation near the critical point), where the subindex 1 means that these symmetry breaking fields have been obtained from the 1-spin cluster, we arrive to the final form of the order parameter in sublattice  $\alpha$

$$\vec{m}_{1\alpha} = \hat{n}_\alpha A(\mathcal{K}') \sum_{\beta \neq \alpha} b_{1\beta}, \quad (27)$$

where

$$A(\mathcal{K}') = z \rho_x^{z(p-1)-1} \nu_x \tanh x|_{x=0}, \quad (28)$$

which, after a straightforward calculation it is found to be

$$A(\mathcal{K}') = \frac{2 \tanh(2\mathcal{K}') + \tanh(4\mathcal{K}')}{4}, \quad (29)$$

for the *kagomé* lattice ( $z = 2$  and  $p = 3$ ), and

$$A(\mathcal{K}') = \frac{5 \tanh(2\mathcal{K}') + 4 \tanh(4\mathcal{K}') + \tanh(6\mathcal{K}')}{16}, \quad (30)$$

for the pyrochlore lattice ( $z = 2$  and  $p = 4$ ).

## B. $p$ -spin cluster order parameter

Let us consider now a cluster formed by  $p$  spins, each of one belonging to a different sublattice (therefore, we will have  $p = 3$  for the *kagomé* lattice and  $p = 4$  for the pyrochlore lattice). The Hamiltonian of such a cluster can be put as

$$\mathcal{H}_p = K \sum_{\alpha \neq \beta} \vec{s}_{1\alpha} \cdot \vec{s}_{1\beta} + \sum_{\alpha} \vec{s}_{1\alpha} \cdot \vec{\xi}_{p\alpha}. \quad (31)$$

In this Hamiltonian, the first term represents the interaction between the spins inside the cluster of size  $p$ , whereas the second term represents the interaction of those same spins with the symmetry breaking fields

$$\vec{\xi}_{p\alpha} = K \sum_{\beta \neq \alpha} \sum_i^{z-1} \vec{s}_{i\beta}, \quad (32)$$

created by the rest of spins outside the cluster. The sum over  $i$  goes over all the NN spins except the ones already included in the cluster. The order parameter for each of the sublattices included in the cluster, obtained from the  $p$ -spin cluster can be now put as

$$\vec{m}_{p\alpha} = \left\langle \frac{Tr_{1A,1B,1C...} \vec{s}_{1\alpha} e^{\mathcal{H}_p}}{Tr_{1A,1B,1C...} e^{\mathcal{H}_p}} \right\rangle_{\mathcal{H}}, \quad (33)$$

or, more conveniently

$$m_{p\alpha}^\mu = \left\langle \frac{\partial}{\partial \xi_{p\alpha}^\mu} \ln Tr_{1A,1B,1C...} e^{\mathcal{H}_p} \right\rangle_{\mathcal{H}}. \quad (34)$$

In these expressions,  $Tr_{1A,1B,1C...}$  represents the trace over the spin degrees of freedom in the  $p$ -spin cluster.

Even though the discussion can be continued for a cluster with an arbitrary number of spins, the mathematical details get very cumbersome. Therefore, we will carry on separately the calculation of the order parameter for the *kagomé* and the pyrochlore lattices.

### 1. *Kagomé* lattice

In the case of the *kagomé* lattice, we will consider a triangular cluster defined by  $p = 3$  spins. In doing so, we can easily calculate the reduced partition function appearing in (34)

$$Tr_{1A,1B,1C} e^{\mathcal{H}_p} = Z_3(\mathcal{K}, \Pi_A, \Pi_B, \Pi_C) = \cosh(\Pi_A + \Pi_B + \Pi_C) + e^{-4\mathcal{K}} [\cosh(\Pi_A - \Pi_B + \Pi_C) + \cosh(\Pi_A + \Pi_B - \Pi_C) + \cosh(\Pi_A - \Pi_B - \Pi_C)], \quad (35)$$

where  $\Pi_\alpha = \hat{n}_\alpha \cdot \vec{\xi}_{3\alpha}$  and  $\mathcal{K} = K \cosh \theta$ . Taking into account the relation

$$\frac{\partial}{\partial \xi_{3\alpha}^\mu} \Pi_\alpha = n_\alpha^\mu, \quad (36)$$

we obtain the expression of the order parameter for the 3-spin cluster

$$\vec{m}_{3\alpha} = \left\langle \frac{\sinh(\Pi_A + \Pi_B + \Pi_C) + e^{-4\mathcal{K}} [\pm \sinh(\Pi_A - \Pi_B + \Pi_C) + \sinh(\Pi_A + \Pi_B - \Pi_C) + \sinh(\Pi_A - \Pi_B - \Pi_C)]}{Z_3(\mathcal{K}, \Pi_A, \Pi_B, \Pi_C)} \right\rangle_{\mathcal{H}} \hat{n}_\alpha, \quad (37)$$

where the  $+$  or  $-$  sign corresponds to the sign of  $\Pi_\alpha$  in the argument of the corresponding  $\sinh$ . To quote an example, the order parameter in sublattice  $B$  is given by

$$\vec{m}_{3B} = \left\langle \frac{\sinh(\Pi_A + \Pi_B + \Pi_C) + e^{-4\mathcal{K}} [-\sinh(\Pi_A - \Pi_B + \Pi_C)]}{Z_3(\mathcal{K}, \Pi_A, \Pi_B, \Pi_C)} + \frac{+\sinh(\Pi_A + \Pi_B - \Pi_C) - \sinh(\Pi_A - \Pi_B - \Pi_C)}{Z_3(\mathcal{K}, \Pi_A, \Pi_B, \Pi_C)} \right\rangle_{\mathcal{H}} \hat{n}_B, \quad (38)$$

By making use again of the operator identity (20), we can express the order parameters as

$$\vec{m}_{3\alpha} = \hat{n}_\alpha \langle e^{\Pi_A D_x} e^{\Pi_B D_y} e^{\Pi_C D_z} \rangle_{\mathcal{H}} g_\alpha(x, y, z)|_{x=y=z=0}, \quad (39)$$

where  $g_\alpha(x, y, z)$  is obtained by making the substitutions  $\Pi_A \rightarrow x$ ,  $\Pi_B \rightarrow y$ , and  $\Pi_C \rightarrow z$  in (37). For example

$$g_B(x, y, z) = \frac{\sinh(x + y + z) + e^{-4\mathcal{K}} [-\sinh(x - y + z) + \sinh(x + y - z) - \sinh(x - y - z)]}{\cosh(x + y + z) + e^{-4\mathcal{K}} [\cosh(x - y + z) + \cosh(x + y - z) + \cosh(x - y - z)]}. \quad (40)$$

By expanding the exponentials of sums in (39) as products of exponentials, and making use again of the van der Waerden identity and the decoupling of the correlations, we arrive, to first order in the symmetry breaking fields  $b_{3\alpha} = \langle s_{i\alpha} \rangle_{\mathcal{H}}$ , to the following system of equations

$$\vec{m}_{3\alpha} = [B_1(\mathcal{K}) b_{3\alpha} + B_2(\mathcal{K})(b_{3\beta} + b_{3\gamma})] \hat{n}_\alpha, \quad (\alpha \neq \beta \neq \gamma), \quad (41)$$

where

$$B_1(\mathcal{K}) = \rho_x^2 \rho_y \rho_z (\nu_y \rho_z + \rho_y \nu_z) g_A(x, y, z)|_{x=y=z=0}, \quad (42)$$

and

$$B_2(\mathcal{K}) = \rho_y^2 \rho_x \rho_z (\nu_x \rho_z + \rho_x \nu_z) g_A(x, y, z)|_{x=y=z=0}, \quad (43)$$

with  $\rho_\mu = \cosh(\mathcal{K} D_\mu)$  and  $\nu_\mu = \sinh(\mathcal{K} D_\mu)$ ,  $\mu = x, y, z$ . After applying the differential operators in the previous expressions, we arrive to the final form for these coefficients

$$B_1(\mathcal{K}) = \frac{1}{12} \left[ \left( \frac{1}{2 \cosh(4\mathcal{K}) + 3e^{-4\mathcal{K}} - 1} + \frac{3}{\cosh(4\mathcal{K}) + e^{-4\mathcal{K}}(2 + \cosh(4\mathcal{K}))} - \frac{6e^{-4\mathcal{K}}}{1 + e^{-4\mathcal{K}}(1 + 2 \cosh(4\mathcal{K}))} \right) \sinh(4\mathcal{K}) + \frac{4 \tanh(2\mathcal{K})}{1 + 3e^{-4\mathcal{K}}} \right], \quad (44)$$

$$B_2(\mathcal{K}) = \frac{1}{24} \left[ \left( \frac{2}{2 \cosh(4\mathcal{K}) + 3e^{-4\mathcal{K}} - 1} + \frac{3(2 + e^{-4\mathcal{K}})}{\cosh(4\mathcal{K}) + e^{-4\mathcal{K}}(2 + \cosh(4\mathcal{K}))} + \frac{3e^{-4\mathcal{K}}}{1 + e^{-4\mathcal{K}}(1 + 2 \cosh(4\mathcal{K}))} \right) \sinh(4\mathcal{K}) + \frac{4(2 + 3e^{-4\mathcal{K}}) \tanh(2\mathcal{K})}{1 + 3e^{-4\mathcal{K}}} \right], \quad (45)$$

Certainly, it is not obvious to see the behavior of  $B_1$  and  $B_2$  from the above expressions, for they are depicted in Fig. 4.

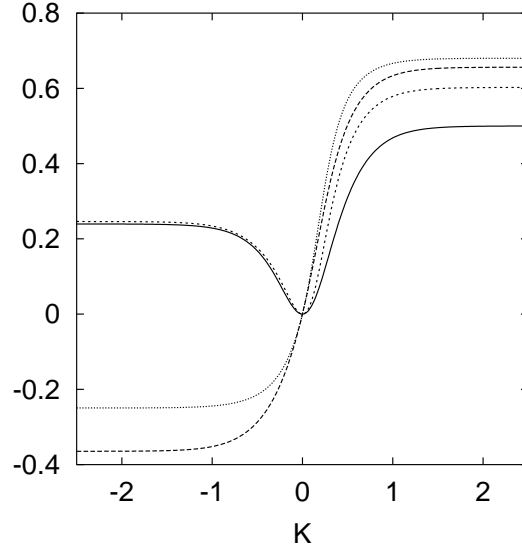


FIG. 4:  $\mathcal{K}$  dependence of  $B_1(\mathcal{K})$  (solid line),  $B_2(\mathcal{K})$  (long dashed line),  $C_1(\mathcal{K})$  (short dashed line), and  $C_2(\mathcal{K})$  (dotted line), given by (42), (43), (49), and (50), respectively.

## 2. Pyrochlore lattice.

The only difference with the previous case is that the cluster contains  $p = 4$  spins, corresponding to 4 different sublattices ( $A, B, C$ , and  $D$ ). Therefore, we will not present the details of the calculation here, but only the main results.

The reduced partition function is given in this case by

$$\begin{aligned}
 Z_4(\mathcal{K}, \Pi_A, \Pi_B, \Pi_C, \Pi_D) = & \cosh(\Pi_A + \Pi_B + \Pi_C + \Pi_D) \\
 & + e^{-6\mathcal{K}} [\cosh(\Pi_A - \Pi_B + \Pi_C + \Pi_D) + \cosh(\Pi_A + \Pi_B - \Pi_C + \Pi_D) \\
 & + \cosh(\Pi_A + \Pi_B + \Pi_C - \Pi_D) + \cosh(\Pi_A - \Pi_B - \Pi_C - \Pi_D)] \\
 & + e^{-8\mathcal{K}} [\cosh(\Pi_A - \Pi_B - \Pi_C + \Pi_D) + \cosh(\Pi_A - \Pi_B + \Pi_C - \Pi_D) \\
 & + \cosh(\Pi_A + \Pi_B - \Pi_C - \Pi_D)], \quad (46)
 \end{aligned}$$

where the definition of  $\Pi_\alpha$  is as given above.

The expression of the order parameter for this cluster is given by

$$\begin{aligned}
 \vec{m}_{4\alpha} = & \left[ \frac{\sinh(\Pi_A + \Pi_B + \Pi_C + \Pi_D)}{Z_4(\mathcal{K}, \Pi_A, \Pi_B, \Pi_C, \Pi_D)} \right. \\
 & + e^{-6\mathcal{K}} \left( \frac{\pm \sinh(\Pi_A - \Pi_B + \Pi_C + \Pi_D) \pm \sinh(\Pi_A + \Pi_B - \Pi_C + \Pi_D)}{Z_4(\mathcal{K}, \Pi_A, \Pi_B, \Pi_C, \Pi_D)} \right. \\
 & \left. + \frac{\pm \sinh(\Pi_A + \Pi_B + \Pi_C - \Pi_D) \pm \sinh(\Pi_A - \Pi_B - \Pi_C - \Pi_D)}{Z_4(\mathcal{K}, \Pi_A, \Pi_B, \Pi_C, \Pi_D)} \right) \\
 & + e^{-8\mathcal{K}} \left( \frac{\pm \sinh(\Pi_A - \Pi_B - \Pi_C + \Pi_D) \pm \sinh(\Pi_A - \Pi_B + \Pi_C - \Pi_D)}{Z_4(\mathcal{K}, \Pi_A, \Pi_B, \Pi_C, \Pi_D)} \right. \\
 & \left. \left. + \frac{\pm \sinh(\Pi_A + \Pi_B - \Pi_C - \Pi_D)}{Z_4(\mathcal{K}, \Pi_A, \Pi_B, \Pi_C, \Pi_D)} \right) \right] \hat{n}_\alpha, \quad (47)
 \end{aligned}$$

where, as before, the  $+$  or  $-$  sign corresponds to the sign of the corresponding  $\Pi_\alpha$  in the argument of the  $\sinh$ .

By making use of the operator identity (20), the van der Waerden identity, and the decoupling approximation, we arrive to the expression of the 4-spin cluster order parameter up to first order in the symmetry breaking fields  $b_{4\alpha} = \langle s_{i\alpha} \rangle_{\mathcal{H}}$ , which is given by the system of equations

$$\vec{m}_{4\alpha} = [C_1(\mathcal{K}) b_{4\alpha} + C_2(\mathcal{K}) (b_{4\beta} + b_{4\gamma} + b_{4\delta})] \hat{n}_\alpha, \quad (\alpha \neq \beta \neq \gamma \neq \delta), \quad (48)$$

where

$$C_1(\mathcal{K}) = \rho_x^3 \rho_y^2 \rho_z^2 \rho_u^2 (\nu_y \rho_z \rho_u + \rho_y \nu_z \rho_u + \rho_y \rho_z \nu_u) g_A(x, y, z, u)|_{x=y=z=u=0}, \quad (49)$$

and

$$C_2(\mathcal{K}) = \rho_x^2 \rho_y^3 \rho_z^2 \rho_u^2 (\nu_x \rho_z \rho_u + \rho_x \nu_z \rho_u + \rho_x \rho_z \nu_u) g_A(x, y, z, u)|_{x=y=z=u=0}. \quad (50)$$

The function  $g_\alpha(x, y, z, u)$  is obtained from the coefficient of  $\hat{n}_\alpha$  in (47) with the substitutions  $\Pi_A \rightarrow x$ ,  $\Pi_B \rightarrow y$ ,  $\Pi_C \rightarrow z$ , and  $\Pi_D \rightarrow u$ .

The evaluation of  $C_1$  and  $C_2$  is straightforward, though rather lengthy, and the final expressions are of little use, due to their length. For that reason, we have preferred not to quote them here, but illustrate their behavior by Fig. 4.

#### IV. SCALING RELATIONS AND CRITICAL BEHAVIOR

Let us summarize the results obtained so far. The order parameters of each sublattice for the 1-spin cluster are related by the system of equations

$$\vec{m}_{1\alpha} = A(\mathcal{K}') \sum_{\beta \neq \alpha} b_{1\beta} \hat{n}_\alpha, \quad (51)$$

whereas the order parameters of each sublattice for the  $p$ -spin cluster are related by the equations

$$\vec{m}_{p\alpha} = \left[ \Phi(\mathcal{K}) b_{p\alpha} + \Theta(\mathcal{K}) \sum_{\beta \neq \alpha} b_{p\beta} \right] \hat{n}_\alpha, \quad (52)$$

where  $A(\mathcal{K}')$ ,  $\Phi(\mathcal{K})$ , and  $\Theta(\mathcal{K})$ , are given by expressions (29), (44), (45), and (30), (49), (50), for the *kagomé* and pyrochlore lattices, respectively.

By making use of the scaling hypothesis (6) for both the order parameter and the symmetry breaking fields<sup>12</sup> we arrive to a system of equations for the symmetry breaking fields

$$\Phi(\mathcal{K}) b_{p\alpha} + [\Theta(\mathcal{K}) - A(\mathcal{K}')] \sum_{\beta \neq \alpha} b_{p\beta} = 0, \quad (53)$$

where  $\Phi$ ,  $\Theta$ , and  $A$  are to be replaced by the corresponding expressions, and  $\alpha, \beta = A, B$ , and  $C$  for the *kagomé* lattice and  $\alpha, \beta = A, B, C$ , and  $D$  for the pyrochlore lattice. This homogeneous system has a non trivial solution if its characteristic determinant is zero, which gives the condition

$$[(p-1)A(\mathcal{K}') - \Phi(\mathcal{K}) - (p-1)\Theta(\mathcal{K})] [A(\mathcal{K}') + \Phi(\mathcal{K}) - \Theta(\mathcal{K})]^{p-1} = 0, \quad (54)$$

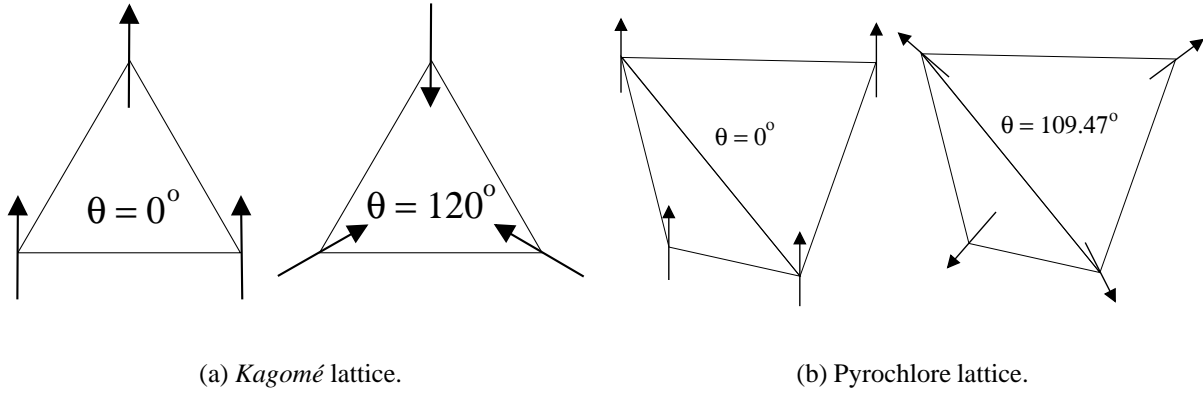


FIG. 5: Type A configuration for the *kagomé* and pyrochlore lattices at  $T = 0$ . The  $\theta = 0$  case corresponds to the standard Ising model, whereas  $\theta \neq 0$  corresponds to anisotropic Ising interactions (see text).

which has two solutions that give us the corresponding RG recursion relations for the coupling constants.

The first one corresponds to

$$\Phi(\mathcal{K}) + (p - 1)\Theta(\mathcal{K}) = (p - 1)A(K'). \quad (55)$$

In this case, the solution of the system of equations is given by (notice that we have omitted the index corresponding to the size of the cluster)

$$b_A = b_B = b_C = \dots \quad (56)$$

or, in terms of the modulus of the order parameter,

$$m_A = m_B = m_C = \dots, \quad (57)$$

and corresponds to a configuration in which all the spins point “out” or all the spins point “in”, as has been depicted in Fig. 5. We will term this configuration “Type A”.

The second solution occurs if

$$\Theta(\mathcal{K}) - \Phi(\mathcal{K}) = A(K'), \quad (58)$$

which leads to a configuration in which

$$\sum_{\alpha} b_{\alpha} = 0, \quad (59)$$

or, in terms of the order parameters

$$\sum_{\alpha} m_{\alpha} = 0. \quad (60)$$

We will term this configuration as “Type B”.

It is important to notice that through the introduction of the effective couplings  $\mathcal{K}'$  and  $\mathcal{K}$ , we can consider both the standard Ising Hamiltonian in these geometries and the corresponding

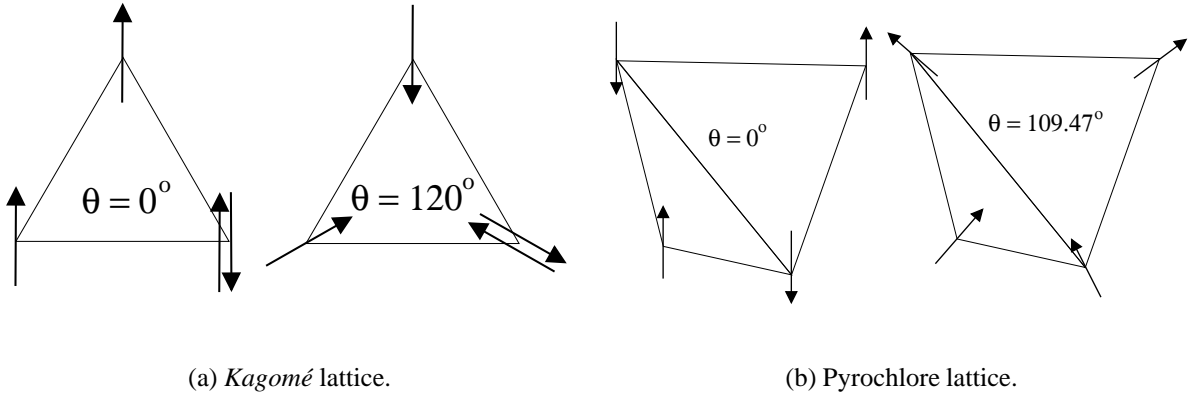


FIG. 6: Type B configuration for the *kagomé* and pyrochlore lattices at  $T = 0$ . The  $\theta = 0$  case corresponds to the standard antiferromagnetic Ising model, whereas  $\theta \neq 0$  corresponds to anisotropic Ising interactions (see text).

spin ice problem on equal footing or, equivalently, we can map the spin ice problem in these geometries to the standard Ising model. Indeed, the standard Ising model corresponds to taking  $\cos \theta = \hat{n}_\alpha \cdot \hat{n}_\beta = 1$ , that is, the spins point along the same direction, whereas the case  $\theta = 120^\circ$  for the *kagomé* lattice corresponds to the 2D spin ice analog commented above. The case  $\theta = 109.47^\circ$  is the spin ice problem in the pyrochlore lattice.

In the case  $\theta = 0^\circ$ , the Type A configuration corresponds to ferromagnetic order, whereas the Type B configuration is a generalization of antiferromagnetic order. Moreover, in the pyrochlore case, and for Ising spins pointing along  $\langle 1, 1, 1 \rangle$ -type directions, the last configuration contains, among others more general, the ground state configuration of the spin ice system, in which two spins point “in” and two spins point “out” (see Fig. 6), and reflects the degeneracy of the ground state due to the geometrical frustration. It is important to notice that it is impossible to satisfy condition (60) in the *kagomé* case at  $T = 0$ , which has been noted in Fig. 6 by a double spin in one of the corners.

Of course, apart from obtaining the possible spin configurations, it is even more important to study if they are thermally stable, that is, if they really occur. To this end, we have to see if there is any value  $\mathcal{K}' = \mathcal{K} = \mathcal{K}_c$  that satisfies conditions (55) and (58), that is, if the RG recursion relations defined by (55) and (58) have any non-trivial fixed points. The simplest way of solving these equations is by using graphical methods, as has been done in Figs. 7 and 8 for the *kagomé* and pyrochlore lattices, respectively.

From these figures, we can see that for the Type B configuration, the only fixed point of the RG transformation is the trivial one, corresponding to a paramagnetic configuration ( $\mathcal{K} = \mathcal{K}' = 0$ ). However, there is a non trivial fixed point for the Type A configuration ( $\mathcal{K}_c = 0.415$  for the *kagomé* lattice and  $\mathcal{K}_c = 0.23$  for the pyrochlore lattice), depending on the sign of the effective coupling or, in other words, depending on whether the effective coupling is ferro- or antiferromagnetic. These results have been collected in Table I, for both the *kagomé* and pyrochlore lattices, and for both the standard Ising model and the spin ice problem. Also, the exact results known for the *kagomé* lattice<sup>13</sup> and the ones obtained from MC data for the pyrochlore lattice<sup>7</sup> are quoted for comparison. It can be seen that the estimates obtained from this RG scheme are in very good agreement with the exact values, in spite of the crudeness of the decoupling approximation and the fact that we have considered clusters of small size. This reflects the well known fact that, in

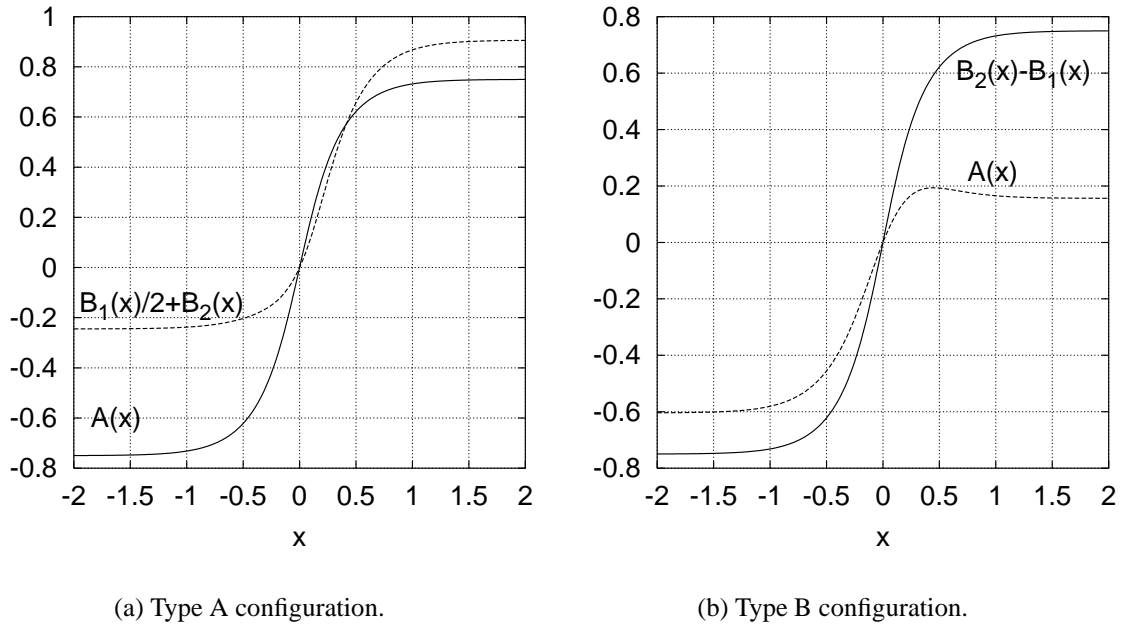


FIG. 7: Graphical estimation of the fixed points of the RG transformation for the *kagomé* lattice.  $A(x)$  is given by (29), whereas  $B_1(x)$  and  $B_2(x)$  are given by (42) and (43), respectively.

$\mathcal{K}_c$	<i>Kagomé</i> Pyrochlore	
EFRG	0.415	0.230
GCC	0.402	0.227
Exact	0.4643 <sup>a</sup>	0.25 <sup>b</sup>

<sup>a</sup>Ref. 13

<sup>b</sup>Ref. 7

TABLE I: Non-trivial fixed points of the RG transformation, and corresponding critical points in the GCC approach (see text).

this GFAF systems, correlations extending outside the frustrated unit are relatively small<sup>20,21</sup>. On the other hand, correlations inside the unit are considered to some extent by the present technique. In any case, the quality of the estimates can be systematically improved by considering larger units as, in this way, we include further correlations. However, the improvement in the estimate of the critical point is not commensurate with the additional algebraic difficulty involved. Another important point is that the EFRG method distinguishes among the various different geometries for a given number of NN, in contrast with standard MF approaches, which do not distinguish, for example between a cubic lattice and a pyrochlore one<sup>32</sup>.

Regarding the question of geometrical frustration, which leads to the absence of a transition to a long range ordered state at any finite temperature, both the *kagomé* and pyrochlore ferromagnetic Ising lattices are non-frustrated, whereas the corresponding antiferromagnetic ones are frustrated, and remain paramagnetic down to 0 K. In the spin ice case ( $\theta = 120^\circ$  for the *kagomé* lattice and  $\theta = 109.47^\circ$  for the pyrochlore), however, the ferromagnetic case is frustrated, and does not order at any finite temperature, whereas the antiferromagnetic one experiments a transition to a



		<i>Kagomé</i>		Pyrochlore	
		$K > 0$	$K < 0$	$K > 0$	$K < 0$
EFRG	$\theta = 0$	0.415	—	0.230	—
	$\theta = 120^\circ (109.47^\circ)$	—	-0.830	—	-0.690
GCC	$\theta = 0$	0.402	—	0.227	—
	$\theta = 120^\circ (109.47^\circ)$	—	-0.804	—	-0.671

TABLE II: Critical points obtained from the EFRG and GCC methods for the Ising, *kagomé* spin ice, and spin ice pyrochlore. The long dashes indicate the absence of a critical point.

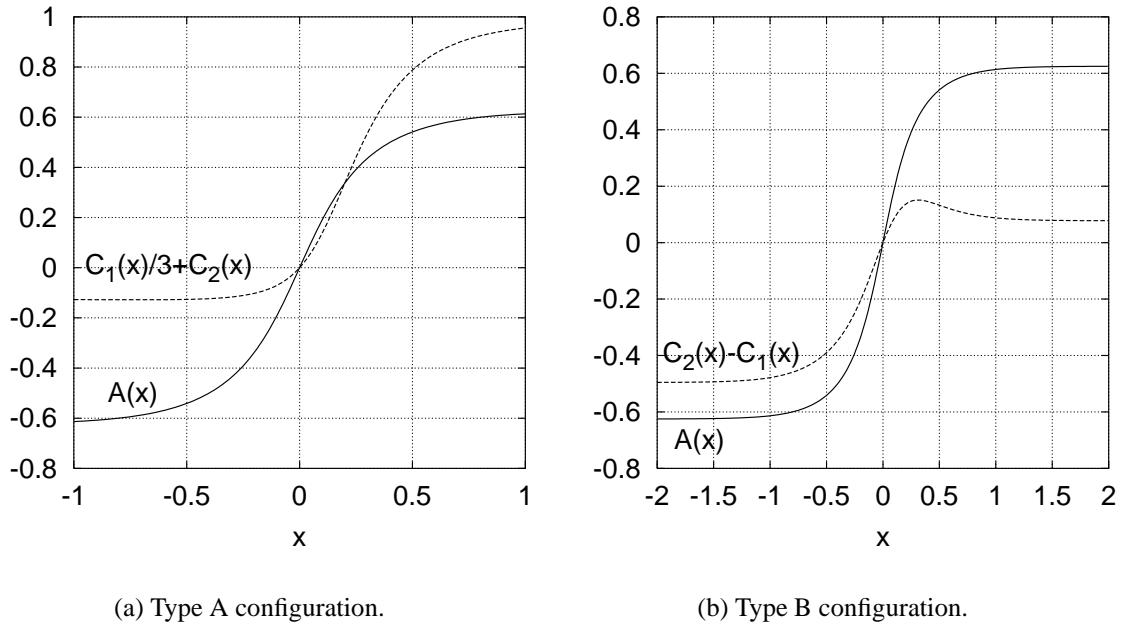


FIG. 8: Graphical estimation of the fixed points of the RG transformation for the pyrochlore lattice.  $A(x)$  is given by (30), whereas  $C_1(x)$  and  $C_2(x)$  are given by (49) and (50), respectively.

long range ordered state at a finite temperature (see Table II). In any case, the ground state given by the “ice rule”<sup>7,9</sup> never occurs in these systems. Furthermore, we can see now that the reason why the ferromagnetic spin ice system is frustrated is that it can be mapped to the standard Ising Hamiltonian with antiferromagnetic effective interaction,  $\mathcal{K} < 0$ , which is known to be frustrated.

## V. CALCULATION OF THE CRITICAL EXPONENTS

In this section we will carry out the calculation of the critical exponents associated with the transition to the Type A configuration, which, as found in the previous section, is the only one that occurs in these systems. As it is easy to see from the considerations in Section II, in order to obtain these exponents, we will need to include the effect of a magnetic field applied to the system, which is what we do in the following.

We can make use of the results of the previous sections to consider the inclusion of the applied magnetic field,  $\vec{h} = h \hat{n}$ , in the direction given by the normal vector  $\hat{n}$ , by redefining the conjugated fields  $\vec{\xi}_{p\alpha}$  as

$$\vec{\xi}_{p\alpha} \rightarrow \vec{\xi}_{p\alpha} + (\hat{n} \cdot \hat{n}_\alpha) h \quad (61)$$

for the  $p$ -spin cluster and

$$\vec{\xi}_{1\alpha} \rightarrow \vec{\xi}_{1\alpha} + (\hat{n} \cdot \hat{n}_\alpha) h' \quad (62)$$

for the 1-spin cluster. The magnetic fields for both clusters scale as

$$h' = l^{y_H} h, \quad (63)$$

with  $y_H$  the magnetic critical exponent<sup>16</sup>.

Now, it is straightforward to see that the corresponding order parameter in each sublattice for the 1-spin cluster is given by

$$\vec{m}_{1\alpha} = \hat{n}_\alpha \left\langle \tanh \left[ \hat{n}_\alpha \cdot \left( \vec{\xi}_{1\alpha} + \hat{n} h \right) \right] \right\rangle_{\mathcal{H}}. \quad (64)$$

For small values of  $h$ , we can put

$$\vec{m}_{1\alpha} \simeq \hat{n}_\alpha \left\{ \left\langle \tanh \left[ \hat{n}_\alpha \cdot \vec{\xi}_{1\alpha} \right] \right\rangle + \left\langle \text{sech}^2 \left[ \hat{n}_\alpha \cdot \vec{\xi}_{1\alpha} \right] \right\rangle (\hat{n} \cdot \hat{n}_\alpha) h + \mathcal{O}(h^2) \right\}. \quad (65)$$

By making use of the exponential operator identity together with the van der Waerden identity, we easily obtain, to the lowest order in the fields  $\vec{\xi}$  and  $\vec{h}$

$$\vec{m}_{1\alpha} \simeq \left\{ A(\mathcal{K}') \sum_{\beta \neq \alpha} b_{1\beta} + F(\mathcal{K}') (\hat{n} \cdot \hat{n}_\alpha) h \right\} \hat{n}_\alpha, \quad (66)$$

where  $A(\mathcal{K}')$  is given by (28) and

$$F(\mathcal{K}') = \rho_x^{z(p-1)} \text{sech}^2(x) \Big|_{x=0}. \quad (67)$$

For the *kagomé* lattice ( $z = 2$  and  $p = 3$ )

$$F(\mathcal{K}') = \frac{1}{8} (3 + 4 \text{sech}^2 2\mathcal{K}' + \text{sech}^2 4\mathcal{K}'). \quad (68)$$

For the pyrochlore lattice ( $z = 2$  and  $p = 4$ )

$$F(\mathcal{K}) = \frac{1}{32} (10 + 15 \text{sech}^2 2\mathcal{K} + 6 \text{sech}^2 4\mathcal{K} + \text{sech}^2 6\mathcal{K}). \quad (69)$$

Let us now turn our attention to the 3-spin cluster in the *kagomé* case. We follow exactly the same procedure we have used to arrive to eq. (66), but using the expression for the order parameter of this cluster, eq. (37). Thus, we first expand  $\vec{m}_{3\alpha}$  in powers of  $h$  and  $b_{3\alpha}$ , after the substitution (61) has been done, and make use of the differential operator and van der Waerden identities. In doing so, we arrive at

$$\vec{m}_{3\alpha}(b_{3A}, b_{3B}, b_{3C}, \vec{h}) \simeq \vec{m}_{3\alpha}(b_{3A}, b_{3B}, b_{3C}) + \hat{n}_\alpha (\vec{G}_\alpha(\mathcal{K}) \cdot \vec{h}) + \mathcal{O}(h^2). \quad (70)$$

The first term on the right member of this expression is the same as (41), whereas the second one is new, and the function  $\vec{G}_\alpha(\mathcal{K})$  is given by

$$\vec{G}_\alpha(\mathcal{K}) = \rho_x^2 \rho_y^2 \rho_z^2 \frac{\partial}{\partial \vec{h}} g_\alpha(x + \hat{n}_A \cdot \vec{h}, y + \hat{n}_B \cdot \vec{h}, z + \hat{n}_C \cdot \vec{h}) \Big|_{\vec{h}=\vec{0}}, \quad (71)$$

with  $g_\alpha(x, y, z)$  given as in (39) and (40). For arbitrary  $\hat{n}_A$ ,  $\hat{n}_B$ , and  $\hat{n}_C$ ,  $\vec{G}_\alpha$  will depend on  $\alpha$  in a complicated way. However, in this work, we are only concerned about the cases studied in the previous Section, namely, the standard Ising model,  $\hat{n}_A = \hat{n}_B = \hat{n}_C$ , and the 2D spin ice problem on the *kagomé* lattice, which verifies the property  $\hat{n}_A + \hat{n}_B + \hat{n}_C = \vec{0}$ . In these cases, it is easy to show that

$$\vec{G}_\alpha(\mathcal{K}) = G(\mathcal{K}) \hat{n}_\alpha, \quad (72)$$

where the form of the function  $G(\mathcal{K})$  does depend on whether  $\hat{n}_A = \hat{n}_B = \hat{n}_C$  or  $\hat{n}_A + \hat{n}_B + \hat{n}_C = \vec{0}$ . In the first case (standard Ising model), this function is given by

$$G_I(\mathcal{K}) = \frac{1}{192} \left( 138 - \frac{320}{(1 + e^{4\mathcal{K}})^2} + \frac{704}{1 + e^{4\mathcal{K}}} - \frac{6144}{(3 + e^{4\mathcal{K}})^2} + \frac{768}{3 + e^{4\mathcal{K}}} + \frac{24(-7 + 3e^{4\mathcal{K}})}{(4 - e^{4\mathcal{K}} + e^{8\mathcal{K}})^2} \right. \\ \left. - \frac{8(-6 + e^{4\mathcal{K}})}{4 - e^{4\mathcal{K}} + e^{8\mathcal{K}}} - \frac{3(17 + 11e^{4\mathcal{K}})}{(1 + e^{4\mathcal{K}} + 2e^{8\mathcal{K}})^2} - \frac{3(1 + 80e^{4\mathcal{K}})}{1 + e^{4\mathcal{K}} + 2e^{8\mathcal{K}}} - \frac{48(-13 - 50e^{4\mathcal{K}} + 63e^{8\mathcal{K}})}{(1 + 5e^{4\mathcal{K}} + e^{8\mathcal{K}} + e^{12\mathcal{K}})^2} \right. \\ \left. + \frac{48(-13 + 18e^{4\mathcal{K}} + e^{8\mathcal{K}})}{1 + 5e^{4\mathcal{K}} + e^{8\mathcal{K}} + e^{12\mathcal{K}}} \right), \quad (73)$$

whereas, in the second case (2D spin ice), it is given by

$$G_{SI}(\mathcal{K}) = \text{sech}^2 2\mathcal{K} (533575 + 1162616 \cosh 4\mathcal{K} + 1014592 \cosh 8\mathcal{K} + 774088 \cosh 12\mathcal{K} \\ + 436732 \cosh 16\mathcal{K} + 178200 \cosh 20\mathcal{K} + 47360 \cosh 24\mathcal{K} + 6824 \cosh 28\mathcal{K} + 317 \cosh 32\mathcal{K}) / \\ [1024(3 \cosh 2\mathcal{K} + \cosh 6\mathcal{K} - 2 \sinh 2\mathcal{K})^2 (-2 \cosh 2\mathcal{K} + \sinh 2\mathcal{K})^2 \\ \times (-1 + 5 \cosh 4\mathcal{K} - 3 \sinh 4\mathcal{K})(1 + 3 \cosh 4\mathcal{K} + \sinh 4\mathcal{K})^2] \\ - \text{sech}^2 2\mathcal{K} (440942 \sinh 4\mathcal{K} + 661942 \sinh 8\mathcal{K} + 618862 \sinh 12\mathcal{K} \\ + 385138 \sinh 16\mathcal{K} + 163174 \sinh 20\mathcal{K} + 44430 \sinh 24\mathcal{K} + 6374 \sinh 28\mathcal{K} + 303 \sinh 32\mathcal{K}) / \\ [1024(3 \cosh 2\mathcal{K} + \cosh 6\mathcal{K} - 2 \sinh 2\mathcal{K})^2 (-2 \cosh 2\mathcal{K} + \sinh 2\mathcal{K})^2 \\ \times (-1 + 5 \cosh 4\mathcal{K} - 3 \sinh 4\mathcal{K})(1 + 3 \cosh 4\mathcal{K} + \sinh 4\mathcal{K})^2]. \quad (74)$$

The  $\mathcal{K}$  dependence of these expressions has been depicted in Fig. 9.

The calculation for the pyrochlore lattice is identical to the one of the *kagomé*, though the algebraic details are a little more involved. The final result of the calculation is qualitatively the same as in the *kagomé* case considered above: the magnetization of the 4-spin cluster can be put as

$$\vec{m}_{4\alpha}(b_{4A}, b_{4B}, b_{4C}, b_{4D}, \vec{h}) \simeq \vec{m}_{4\alpha}(b_{4A}, b_{4B}, b_{4C}, b_{4D}) + H(\mathcal{K}) (\hat{n}_\alpha \cdot \vec{h}) \hat{n}_\alpha + \mathcal{O}(h^2). \quad (75)$$

where the first term on the right member is given by (48) and  $H(\mathcal{K})$  is obtained from the  $g_\alpha$  function for the pyrochlore case as

$$\vec{H}_\alpha(\mathcal{K}) = \rho_x^2 \rho_y^2 \rho_z^2 \frac{\partial}{\partial \vec{h}} g_\alpha(x + \hat{n}_A \cdot \vec{h}, y + \hat{n}_B \cdot \vec{h}, z + \hat{n}_C \cdot \vec{h}) \Big|_{\vec{h}=\vec{0}}, \quad (76)$$

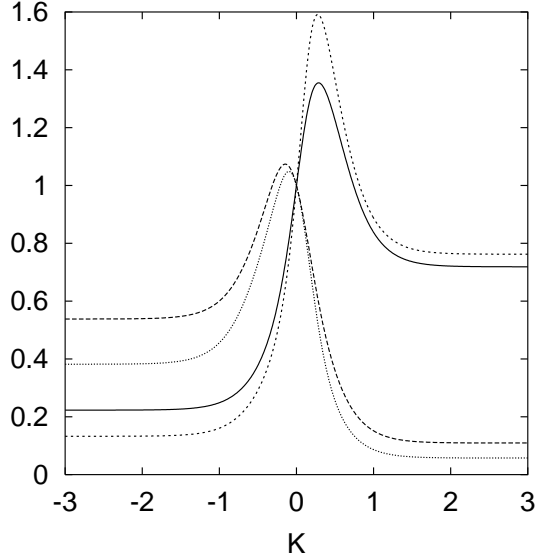


FIG. 9:  $\mathcal{K}$  dependence of the functions  $G_I(\mathcal{K})$  (solid line),  $G_{SI}(\mathcal{K})$  (long dashed line) (given by (73) and (74), respectively),  $H_I(\mathcal{K})$  (short dashed line), and  $H_{SI}(\mathcal{K})$  (dotted line), (obtained from (76), see text).

Again, for the cases considered in this work,  $\hat{n}_A = \hat{n}_B = \hat{n}_C = \hat{n}_D$  (standard Ising) or  $\hat{n}_A + \hat{n}_B + \hat{n}_C + \hat{n}_D = \vec{0}$  (spin ice), it can be easily shown that  $\vec{H}_\alpha(\mathcal{K}) = H(\mathcal{K}) \hat{n}_\alpha$ , where the form of the function  $H(\mathcal{K})$  does depend on whether we are considering the standard Ising or the spin ice problem. We will represent by  $H_I(\mathcal{K})$  the first possibility and by  $H_{SI}(\mathcal{K})$  the second. The length of these expressions makes them of little practical use and, therefore, we will not quote them here. It is enough for our purposes to give their  $\mathcal{K}$  dependence by means of Fig. 9.

Now, by using the scaling relation (4), we can equate the results for the 1-spin cluster with those for the  $p$ -spin cluster, as we did in Sec. IV. In doing so, we obtained the following system of equations for the internal fields

$$\Phi(\mathcal{K}) b_{p\alpha} + [\Theta(\mathcal{K}) - A(\mathcal{K}')] \sum_{\beta \neq \alpha} b_{p\beta} = [F(\mathcal{K}') l^{-d+2y_H} - \Xi(\mathcal{K})] (\hat{n}_\alpha \cdot \hat{n}) h, \quad (77)$$

where  $\Phi(\mathcal{K})$ ,  $\Theta(\mathcal{K})$ , and  $A(\mathcal{K})$  are the same as in Sec. IV,  $F(\mathcal{K}')$  is given by (68) and (69), for the *kagomé* and pyrochlore lattices, respectively, and  $\Xi(\mathcal{K})$  is given by  $G(\mathcal{K})$  ( $G_I(\mathcal{K})$  for the standard Ising model, and  $G_{SI}(\mathcal{K})$  for the 2D spin ice) for the *kagomé* lattice, and  $H(\mathcal{K})$  ( $H_I(\mathcal{K})$  for the standard Ising model, and  $H_{SI}(\mathcal{K})$  for the spin ice) for the pyrochlore lattice.

In the limit case  $h = 0$ , we recover the results obtained in Section IV for the critical point. However, now we have an additional relation that allows us to evaluate the magnetic critical exponent as

$$y_H = \frac{1}{2} \left[ d + \frac{1}{\ln l} \ln \frac{\Xi(\mathcal{K}_c)}{F(\mathcal{K}_c)} \right]. \quad (78)$$

Moreover, the correlation length critical exponent is calculated by making use of (12) and (13) as

$$\nu = \frac{\ln l}{\ln \lambda_T}, \quad (79)$$

	<i>Kagomé</i>		Pyrochlore	
	$\nu$	$y_H$	$\nu$	$y_H$
Standard Ising ( $\hat{n}_A = \hat{n}_B = \dots$ )	1.07	1.64	0.83	2.32
Spin Ice ( $\sum_{\alpha} \hat{n}_{\alpha} = \vec{0}$ )	1.07	0.63	0.83	1.22
Exact (Standard Ising) <sup>a</sup>	1	1.875	0.63	2.48

<sup>a</sup>Refs. 22,23,24,25

TABLE III: Values of the critical exponents.

where

$$\lambda_T = \left[ \frac{\partial}{\partial K} (\Phi(K) + (p-1)\Theta(K)) \right] \left[ (p-1) \frac{\partial}{\partial K'} A(K') \right]^{-1} \Big|_{K_c}. \quad (80)$$

The values of  $\nu$  and  $y_H$  obtained for both standard Ising spins and spin ice spins, and for both the *kagomé* and the pyrochlores lattices, are quoted in Table III. The other exponents for the different thermodynamic quantities can be obtained from these by making use of the well known scaling relations<sup>16</sup> (see Table IV). The values listed as “exact” are those obtained for the square and cubic lattices, as they are expected to be the same as for the *kagomé* and pyrochlore lattices, respectively, on the basis of the universality hypothesis. The ones corresponding to the square lattice are those obtained from the Onsager solution<sup>22</sup>, whereas the ones for the cubic lattice are values obtained from high-precision numerical studies<sup>23,24,25</sup>.

The first conclusion we can extract from the listed values for the standard Ising problem is that the EFRG method provides very reliable estimates for the critical exponents, in spite of the fact that we have chosen the smallest possible clusters that include the effects of frustration. In this sense, the exponents calculated in this work are some of the “best” that can be found in the literature, calculated in the framework of phenomenological RG approaches. For example, the exponents obtained in our work are even better than the ones obtained in the so called Mean Field RG method for Ising spins in the square lattice, where clusters of 16 and 25 spins were used<sup>12</sup>. The reason for this improvement is in the use of the van der Waerden identity, which exactly takes into account the value of the autocorrelation function. It is also important to note that the estimation of  $\nu$  for the *kagomé* lattice is better than the one for the pyrochlore lattice. The reason is that the scaling factor we have used,  $l = (N/N')^{1/d} = p^{1/d}$ , is smaller for the 3D lattice than for the 2D one. It has been noted by some authors, that the values of the critical exponents calculated with this method can be improved by using an alternative definition of the size of the clusters, in terms of the number of interactions including the ones with the spins creating the effective field<sup>26</sup>. This point will be further investigated in a future work<sup>33</sup>.

The last important conclusion we can extract from Table III is that the magnetic critical exponent and, thus, all the exponents depending on this one ( $\beta$ ,  $\gamma$ ,  $\delta$ , and  $\eta$ ), are *different for the spin ice case*. If we take into account the good agreement found for the standard Ising case, we can expect the estimations of the critical exponents for the spin ice case to be of the same quality. Actually, if we assume that the error in the determination of the critical exponents for the spin ice case is the same as in the standard Ising case ( $\Delta y_H/y_H = 0.13$  for the *kagomé* Ising case and  $\Delta y_H/y_H = 0.06$  for the pyrochlore Ising), and we see no reason for this not to be the case, we can put an upper and lower bounds for the real value of this exponent,  $y_H = 0.63 \pm 0.08$  for the *kagomé* spin ice, and  $y_H = 1.22 \pm 0.07$  for the pyrochlore spin ice. Apart from a possible relative

Critical exponent	Scaling relation
$\alpha$	$2 - d/y_H$
$\beta$	$(d - y_H)/y_T$
$\gamma$	$(2y_H - d)/y_T$
$\delta$	$y_H/(d - y_H)$
$\eta$	$2 - 2y_H + d$
$\nu$	$1/y_t$

TABLE IV: Expressions of the critical exponents in terms of the RG critical exponents  $y_T$  and  $y_H$ .

error of about a 10% in the worse case, they are obviously very different from the  $y_H$  of the standard Ising model and, in fact, we have not found in the literature any reference to any other system with these values for  $y_H$ . A *naive* interpretation of these exponents could make us think that our results violate the universality hypothesis. However, it is easy to realize that this is not the case. Indeed, the universality hypothesis states that the critical exponents are the same for different systems with Hamiltonians which internal symmetries are the same, independently of details as the microscopic origin of the interactions or the geometry of the lattice. The results we found for the standard Ising model in both the *kagomé* and pyrochlore lattices are in good agreement with this idea. Moreover, the fact that the thermal exponent does not change when going from Ising spins with a single anisotropy axis, to the spin ice problem, is also in agreement with the universality hypothesis, as we have previously shown that the spin ice problem maps on an Ising Hamiltonian with effective interactions given by  $\mathcal{K} = K \cos \theta$ . However, when we include the effect of an uniform magnetic field in the spin ice case, the Zeeman term cannot be mapped to the Zeeman term in the Ising Hamiltonian with a single anisotropy axis, which is the same for all the spins, but we can see it as a Zeeman which is different for spins located in different sublattices, i.e., it is equivalent to some kind of *staggered* field subject to the condition  $\sum_{\alpha} \vec{h}_{\alpha} = \vec{0}$ , where by  $\vec{h}_{\alpha}$  we represent the magnetic field acting on each sublattice. Certainly, this Zeeman term has not the same symmetry as the original Zeeman term of the Ising spin model with a single anisotropy axis and, therefore, *we should expect the corresponding magnetic critical exponent to be different from the one of the standard Ising model*. Of course, it would be extremely important to have experimental confirmation of this fact, or even estimations of the magnetic critical exponent obtained from high precision Monte Carlo simulations but, as far as we know, this is the first time that this result is reported.

Another interesting point we want to notice here is the connection of these spin ice-like systems with the well known vertex models<sup>7,22</sup>. In fact, it is easy to see that the 2D spin ice of this work is related to the 8-vertex model, whereas the spin ice on the pyrochlore is related to the 16-vertex model. On the other hand, it is well known that these vertex models have the peculiarity that the critical exponents depend continuously on the value of the exchange coupling, and this is precisely what we would expect in our model if we allow for arbitrary orientations of the unit vectors  $\hat{n}_{\alpha}$ , for which  $\hat{n}_A \cdot \hat{n}_B \neq \hat{n}_A \cdot \hat{n}_B \neq \dots$ . We think that clearly establishing this connection, though outside of the scope of this work, deserves further consideration, as it seems that these spin ice-like systems are one of the few physical realizations of these vertex models<sup>34</sup>. In this sense, we think that the present RG scheme could prove to be useful in obtaining qualitative information about critical properties of the 16-vertex model, about which very little is known.

## VI. THE GCC METHOD APPLIED TO THE SPIN ICE PROBLEM

As stated in the Introduction, it is interesting to compare the results obtained in the previous sections with those obtained in the framework of the GCC method, which has been successfully applied to the problem of Heisenberg frustrated lattices by the present authors<sup>14,15</sup>. In the GCC framework, we initially consider isolated units (tetrahedra or triangles, for the pyrochlore and *kagomé* lattices, respectively), and later add the interactions with the surrounding units as unknown effective fields to be determined by a self consistent condition, which is obtained by comparing the order parameter in the cluster with that of the isolated ion<sup>14,27</sup>. We will analyze here the case in which the applied magnetic field is zero, even though the generalization is straightforward.

As in the previous sections, we will characterize each spin in the frustrated unit by a different order parameter. Therefore, the Hamiltonian of the cluster formed by one Ising spin is given by

$$\mathcal{H}_{1\alpha} = 2K \vec{s}_{1\alpha} \sum_{\beta \neq \alpha} \vec{h}_{\beta} = 2\vec{s}_{1\alpha} \cdot \vec{\xi}_{1\alpha}, \quad (81)$$

where  $\vec{h}_{\beta}$  are the internal fields created by the neighboring spins outside the unit, and point along the directions given by  $\hat{n}_{\beta}$ , and we have taken into account that there are 2 neighbors in each sublattice. The Hamiltonian of the cluster formed by  $p$  spins can be put as

$$\mathcal{H}_p = K \sum_{\alpha \neq \beta} \vec{s}_{1\alpha} \cdot \vec{s}_{1\beta} + \sum_{\alpha} \vec{s}_{1\alpha} \cdot \vec{\xi}_{p\alpha}. \quad (82)$$

We can then see that the corresponding partition function of the unit has the same functional form as eqs. (37) and (47) for the *kagomé* and pyrochlore lattices, respectively, except for the fact that the average with respect to the full Hamiltonian is absent, and the conjugated fields  $\vec{\xi}_{\alpha}$  appearing in  $\Pi_{\alpha}$  depend on the internal fields  $\vec{h}_{\beta}$ , rather than on the spin variables of the surrounding spins outside the cluster. As stated above, these internal fields are evaluated by imposing the self consistent condition of equating the magnetization per spin in the internal field with that of a unit in the internal field, which can be mathematically stated as

$$\vec{m}_{1\alpha}(\vec{h}_A, \vec{h}_B, \vec{h}_C, \dots) = \vec{m}_{p\alpha}(\vec{h}_A, \vec{h}_B, \vec{h}_C, \dots). \quad (83)$$

Obviously, this equation can only be solved numerically in the general case. However, near the critical point, we expect the internal fields to be very small, so we can expand the order parameters to first order in the internal fields. In doing so, we obtain

$$m_{1\alpha} \simeq 2\mathcal{K} \sum_{\beta \neq \alpha} h_{\beta}, \quad (84)$$

$$m_{p\alpha} = 2\mathcal{K} \left( A_1(\mathcal{K}) h_{\alpha} + A_2(\mathcal{K}) \sum_{\beta \neq \alpha} h_{\beta} \right), \quad (85)$$

where  $\mathcal{K} = K \cos \theta$ , as before, and

$$A_1(\mathcal{K}) = \begin{cases} \frac{1-e^{-4\mathcal{K}}}{1+3e^{-4\mathcal{K}}} \\ \frac{3(1-e^{-8\mathcal{K}})}{1+4e^{-6\mathcal{K}}+3e^{-8\mathcal{K}}} \end{cases},$$

and

$$A_2(\mathcal{K}) = \begin{cases} \frac{1+e^{-4\mathcal{K}}}{1+3e^{-4\mathcal{K}}} \\ \frac{3+4e^{-6\mathcal{K}}+e^{-8\mathcal{K}}}{1+4e^{-6\mathcal{K}}+3e^{-8\mathcal{K}}} \end{cases}, \quad (86)$$

where the upper (lower) expression corresponds to the *kagomé* (pyrochlore) lattice.

Then, we arrive to the following system of equations for the effective fields

$$\Phi(\mathcal{K}) h_\alpha + \Theta(\mathcal{K}) (h_\beta + h_\gamma + \dots) = 0, \quad (\alpha \neq \beta \neq \gamma \neq \dots), \quad (87)$$

where

$$\Phi(\mathcal{K}) = A_1(\mathcal{K}), \quad (88)$$

and

$$\Theta(\mathcal{K}) = A_2(\mathcal{K}) - \begin{Bmatrix} 1 \\ 2 \end{Bmatrix} = \begin{cases} -\frac{2}{3+e^{4\mathcal{K}}} \\ \frac{1-4e^{-6\mathcal{K}}-5e^{-8\mathcal{K}}}{1+4e^{-6\mathcal{K}}+3e^{-8\mathcal{K}}} \end{cases}. \quad (89)$$

Again, the upper (lower) expression corresponds to the *kagomé* (pyrochlore) lattice.

This system of equations has two non-trivial solutions for

$$\Phi(\mathcal{K}) = \Theta(\mathcal{K}) \quad (90)$$

and

$$\Phi(\mathcal{K}) = -(p-1)\Theta(\mathcal{K}). \quad (91)$$

The first one corresponds to a configuration in which  $\sum_\alpha h_\alpha = 0$ , whereas the second one corresponds to a configuration in which  $h_A = h_B = h_C = \dots$ , that is, they are the same configurations we found in the EFRG formulation. It is easy to verify that the first kind of solution never occurs for any finite value of  $\mathcal{K}$ , whereas the second one occurs for a value of  $\mathcal{K}_c = 0.402$  for the *kagomé* lattice and  $\mathcal{K}_c = 0.227$  for the pyrochlore lattice, in very good agreement with our previous results (see Table I).

## VII. CONNECTION BETWEEN THE GCC AND EFRG SCHEMES

From the previous section, it seems clear that both approaches presented in this work are somehow related. In this section we will furnish this connection. We will consider a system with only one vectorial order parameter. The generalization to an arbitrary number of order parameters being straightforward.

The Hamiltonian of the one spin cluster with only NN interactions can be put as

$$\mathcal{H} = \vec{s}_1 \cdot \vec{\xi}_1 = \vec{s}_1 \cdot \left( K \sum_i^z \vec{s}_i \right), \quad (92)$$

where  $z$  is the number of NN. The corresponding order parameter can be obtained then from the Callen-Suzuki identity and, in general, it will be a function of the conjugated field  $\vec{\xi}_1$

$$\vec{m}_1 = \left\langle \frac{\partial}{\partial \vec{\xi}_1} \ln Z_1(\vec{\xi}_1) \right\rangle_{\mathcal{H}} = \left\langle \vec{F}(\vec{\xi}_1) \right\rangle_{\mathcal{H}} = \left\langle \sum_\mu F_\mu \left( K \sum_i^z \vec{s}_i \right) \hat{n}_\mu \right\rangle_{\mathcal{H}}, \quad (93)$$



where  $\hat{n}_\mu$  define the coordinate system. Obviously, we can expand the function  $\vec{F}$  in powers of  $\vec{s}_i$  as

$$\begin{aligned} \vec{m}_1 &= \sum_\mu \hat{n}_\mu \left\langle F_\mu(\vec{0}) + \sum_i^z \frac{\partial F_\mu}{\partial \vec{s}_i} \Big|_{\vec{s}_i=\vec{0}} \cdot \vec{s}_i + \frac{1}{2!} \sum_{i,j} \frac{\partial^2 F_\mu}{\partial \vec{s}_i \cdot \partial \vec{s}_j} \Big|_{\vec{s}_i=\vec{s}_j=\vec{0}} \vec{s}_i \cdot \vec{s}_j + \dots \right\rangle_{\mathcal{H}} \\ &= \sum_\mu \hat{n}_\mu \left[ F_\mu(\vec{0}) + \sum_i^z \frac{\partial F_\mu}{\partial \vec{s}_i} \Big|_{\vec{s}_i=\vec{0}} \cdot \langle \vec{s}_i \rangle_{\mathcal{H}} + \frac{1}{2!} \sum_{i,j} \frac{\partial^2 F_\mu}{\partial \vec{s}_i \cdot \partial \vec{s}_j} \Big|_{\vec{s}_i=\vec{s}_j=\vec{0}} \langle \vec{s}_i \cdot \vec{s}_j \rangle_{\mathcal{H}} + \dots \right]. \end{aligned} \quad (94)$$

If we now apply the decoupling approximation to this expression

$$\langle s_i^\mu s_j^\nu \dots s_k^\eta \rangle_{\mathcal{H}} \simeq \langle s_i^\mu \rangle_{\mathcal{H}} \langle s_j^\nu \rangle_{\mathcal{H}} \dots \langle s_k^\eta \rangle_{\mathcal{H}} = h_1^\mu h_1^\nu \dots h_1^\eta, \quad (95)$$

where  $\vec{h}_1 = \langle \vec{s}_i \rangle_{\mathcal{H}}$ , and take into account that the variables in the derivatives are dummy variables, that is, we can put

$$\frac{\partial F_\mu(\vec{s}_i)}{\partial \vec{s}_i} \Big|_{\vec{s}_i=\vec{0}} = \frac{\partial F_\mu(\langle \vec{s}_i \rangle)}{\partial \langle \vec{s}_i \rangle} \Big|_{\langle \vec{s}_i \rangle=\vec{0}}, \quad (96)$$

the series can be resummed in terms of the effective internal field  $\vec{h}_1$  to give

$$\vec{m}_1 \simeq \vec{F}(z K \vec{h}_1). \quad (97)$$

Obviously, we can do the same with the  $p$  cluster order parameter, and the result is

$$\vec{m}_p \simeq \vec{G}((z-1) K \vec{h}_p), \quad (98)$$

where  $\vec{h}_p = \langle \vec{s}_i \rangle_{\mathcal{H}}$  is the effective internal field obtained from the  $p$ -spin cluster. We can then easily see that the GCC self consistency condition corresponds to the particular case of the finite size scaling hypothesis in which one assumes

$$\vec{m}_{p'} = \vec{m}_p, \quad (99)$$

and

$$\vec{h}_{p'} = \vec{h}_p. \quad (100)$$

Thus, the GCC model corresponds to the lowest order of the EFRG method, in which correlations outside the cluster are neglected and the scaling relation is substituted by strict equality.

Therefore, the value of the critical point obtained in both methods, to this order of approximation, is the same, as it does not depend on the particular scaling coefficient. However, this has profound consequences for the calculation of other quantities, as the critical exponents, which do depend on the particular scaling relation, as have been noted by some authors<sup>12</sup>. The differences between the values listed in Table I are not related to the use of the EFRG or GCC methods, but to the fact that we have used the van der Waerden identity in the case of the EFRG. However, we could make use of this identity in the GCC approach, at least for Ising spins, and the results would be identical to this order of approximation (i.e. up to terms linear in  $K_c$ ).

It is also important to stress that the results of this section are not limited to the connection between the EFRG and GCC methods applied to GFAF, as we have not made any assumption about the sizes of the clusters. In this sense, this connection also holds for the original formulation of both the Constant Coupling and EFRG methods, in which clusters with 1 and 2 spins are compared<sup>27</sup>. In other words, the Constant Coupling method (in whatever formulation) is the lowest order approximation of the EFRG method, corresponding to neglecting multispin correlations and assuming that the anomalous dimension of the order parameter is zero.

## VIII. CONCLUSIONS

In this work we have studied the critical behavior of ferro- and antiferromagnetically coupled Ising spins with local anisotropy axes in geometrically frustrated geometries (*kagomé* and pyrochlores lattices). The present problem, applied to the pyrochlore lattice with local anisotropy axes in high symmetry  $\langle 111 \rangle$ -like directions corresponds to the spin ice problem. The critical points have been calculated by means of the effective field renormalization group technique, adequately generalized to deal with the non-Bravais character of the lattices, and by the generalized constant coupling approach. These methods allow us to evaluate both the critical points, if any, and the corresponding ground state configurations. The results obtained are in very good agreement with exact results known for the Ising Hamiltonian in the 2D *kagomé* lattice and Monte Carlo calculations for the pyrochlore lattice. For ferromagnetic interactions, geometrical frustration prevents the formation of long range order, whereas for antiferromagnetic ones, there is a transition at a finite temperature to a long range ordered state in which all the spins of the unit point outside or inside the frustrated unit. These results can be traced back to the fact that this spin ice problem can be mapped to the standard Ising model with an effective interaction given by  $\mathcal{K} = K \cos \theta$ , where  $\theta$  is the angle between any 2 anisotropy directions. Therefore, ferromagnetic interactions in the spin ice problem correspond to effective antiferromagnetic ones, and vice versa. Incidentally, the connection between the effective field renormalization group technique and the generalized constant coupling method is furnished. It is shown that the GCC method corresponds to the lowest approximation of the EFRG scheme, in which correlations outside the cluster are neglected and the anomalous dimension of the order parameter is taken to be zero.

In addition, the critical exponents of these systems have been calculated for the transition to the long range ordered state that occurs for effective ferromagnetic interactions. The calculated values of the critical exponents for spins with parallel anisotropy axes (the standard Ising model), are found to be in very good agreement with both those obtained from exact results for the 2D square lattice and those calculated computationally for the cubic lattice, in spite of the small size of the clusters considered in this work. This fact is in agreement with the universality hypothesis. For the spin ice problem (in both the *kagomé* and the pyrochlore lattice), the thermal exponent has the same value as for standard Ising spins, as both Hamiltonians can be identically mapped on to each other. However, the magnetic exponent is found to be different from that of the standard Ising model in the presence of an uniform magnetic field. This result is expected, as the Zeeman term in this case has different symmetry properties than in the standard Ising model. In any case, independent confirmation of this fact, by experimental or Monte Carlo simulations, would be desirable.

We think that the techniques presented in this work will prove to be useful in studying other phenomena present in the spin ice system. For example, it would be interesting to study how the inclusion of long range dipolar interactions modify the present results, that is, if these additional interactions could remove the degeneracy of the ground state so a long range ordered state is formed at any finite temperature for the ferromagnetic case. So far, there are numerical results and mean field calculations which indicate that the degeneracy of the ground state is weakly lifted by long range dipolar interactions, and there is a finite temperature much lower than the energy scale defined by the dipolar interactions at which a long range ordered state given by the ice rules is formed<sup>28,29</sup>, but we think it would be important also to support this result with analytical calculations that go beyond mean field theory. Also, the effect of a small amount of dilution in the crystalline lattice is an intriguing problem which can be dealt with in the present formalisms. Moreover, even though the extension is not trivial, the present EFRG scheme can be generalized to

deal with Heisenberg spins and, thus, shed some light in the fascinating phenomena of geometrical frustration.

Of course, the EFRG scheme is not exempt of limitations. For example, the inclusion of fluctuating corrections coming from correlations further than NN interactions is not an easy task. However, there are some methods to deal with this problem<sup>30</sup>, though they are highly technical and outside of the scope of the present work. This, and some of the problems mentioned in the above paragraph are the directions of our present research.

### Acknowledgments

AJGA wishes to thank the Spanish MEC for financial support under the Subprograma General de Perfeccionamiento de Doctores y Tecnólogos en el Extranjero.

---

\* Electronic address: garcia@landau.physics.wisc.edu

- <sup>1</sup> M. J. P. Gingras, ed., *Proceedings of the Highly Frustrated Magnetism Conference 2000* (to be published).
- <sup>2</sup> A. P. Ramirez, Annual Review of Materials Science **24**, 453 (1994).
- <sup>3</sup> P. Schiffer and A. P. Ramirez, Comments Condens. Mater. Phys. **18**, 21 (1996).
- <sup>4</sup> R. Moessner, in *Proceedings of the Highly Frustrated Magnetism 2000 Conference*, edited by M. J. P. Gingras, (cond-mat/0010301).
- <sup>5</sup> M. J. Harris, S. T. Bramwell, D. F. McMorrow, T. Zeiske, and K. W. Godfrey, Physical Review Letters **79**(13), 2554 (1997).
- <sup>6</sup> M. J. Harris, S. T. Bramwell, P. C. W. Holdsworth, and J. D. M. Champion, Physical Review Letters **81**(20), 4496 (1998).
- <sup>7</sup> S. T. Bramwell and M. J. Harris, J. Phys.: Condens. Matter **10**, L215 (1998).
- <sup>8</sup> R. Moessner, Phys. Rev. B **57**(10), R5587 (1998).
- <sup>9</sup> A. P. Ramirez, C. L. Broholm, R. J. Cava, and G. R. Kowach, Physica B **280**, 290 (2000).
- <sup>10</sup> Z. Y. Li and C. Z. Yang, Physical Review B **37**, 5744 (1988).
- <sup>11</sup> I. P. Fittipaldi, J. Mag. Magn. Mat. **131**, 43 (1994).
- <sup>12</sup> J. A. Plascak, W. Figueiredo, and B. C. S. Grandi, Brazilian Journal of Physics **29**(3), 579 (1999).
- <sup>13</sup> I. Syozi, *Transformation of Ising models* (Academic, London, 1972), vol. 1 of *Phase transitions and critical phenomena*, chap. 7, pp. 269–330.
- <sup>14</sup> A. J. Garcia-Adeva and D. L. Huber, Physical Review B (to be published, cond-mat/0010109).
- <sup>15</sup> A. J. Garcia-Adeva and D. L. Huber, Physical Review B (to be published, cond-mat/0011170).
- <sup>16</sup> N. Goldenfeld, *Lectures on Phase Transitions and the Renormalization Group* (Addison-Wesley, 1994).
- <sup>17</sup> H. B. Callen, Phys. Lett. **4**, 161 (1963).
- <sup>18</sup> M. Suzuki, Phys. Lett. **19**, 267 (1965).
- <sup>19</sup> R. Honmura and T. Kaneyoshi, J. Phys. C **12**, 3979 (1979).
- <sup>20</sup> B. Canals and C. Lacroix, Phys. Rev. Lett. **80**(13), 2933 (1998).
- <sup>21</sup> B. Canals and C. Lacroix, Phys. Rev. B **61**(2), 1149 (2000).
- <sup>22</sup> R. J. Baxter, *Exactly Solved Models in Statistical Mechanics* (Academic, London, 1982).
- <sup>23</sup> D. P. Landau, Physica A **205**, 41 (1994).
- <sup>24</sup> H. W. J. Bloete, E. Luijten, and J. R. Heringa, J. Phys. A **28**, 6289 (1995).

- <sup>25</sup> A. L. Tapalov and H. W. J. Bloete, J. Phys. A **29**, 5727 (1996).
- <sup>26</sup> P. A. Slotte, J. Phys. A **20**, L177 (1987).
- <sup>27</sup> R. J. Elliott, J. Phys. Chem. Solids **16**, 165 (1960).
- <sup>28</sup> M. J. P. Gingras and B. C. den Hertog (cond-mat/0012275).
- <sup>29</sup> R. G. Melko, B. C. den Hertog, and M. J. P. Gingras (cond-mat/0009225).
- <sup>30</sup> X. Jiang and J. Zhong, Phys. Stat. Sol. (b) **193**, K5 (1996).
- <sup>31</sup> It is important to stress that this single axis Ising spin system cannot occur in a pyrochlore lattice, as it is incompatible with the cubic symmetry of the spatial group. However, it is a very instructive example, and will prove to be useful for testing the accuracy of the results presented in this work.
- <sup>32</sup> This is the case even if we consider the smallest possible clusters. See, for example, I. P. Fittipaldi and D. F. de Alburquerque, J. Magn. Magn. Mat. **104-107**, 236 (1992), where they studied the Ising model with bond dilution in both the simple square and *kagomé* lattices in the EFRG framework by using clusters of 1 and 2 spins, respectively.
- <sup>33</sup> Another possible definition of the scaling factor we can use consists in calculating from (79) the value of  $l$  that leads to the exact value of  $y_t$  for the standard Ising model, and make use of this value to estimate the corresponding magnetic critical exponent. The values of  $l$  obtained in this way are  $l = 1.67$  and  $l = 1.42$  for the *kagomé* and pyrochlore lattices, respectively. The corresponding magnetic critical exponents are  $y_H = 1.68$  and  $y_H = 2.58$ , for the standard Ising model in the *kagomé* and pyrochlore lattices, respectively, and  $y_H = 0.60$  and  $y_H = 1.13$ , for the 2D spin ice and the 3D spin ice, respectively.
- <sup>34</sup> Even though this is only the case for very special cases, as the ones considered in this work, because spin ice systems with arbitrary unitary vectors are, in general, incompatible with the symmetries of the crystalline lattice.